Experimental study of harmonic generation from solid surfaces irradiated by multipicosecond laser pulses

R. A. Ganeev,[1] J. A. Chakera,[2] and M. Raghuramaiah,[2] A. K. Sharma,[2] P. A. Naik,[2] and P. D. Gupta[2]
[1]*NPO Akadempribor, Tashkent 700 143, Uzbekistan*
[2]*Centre for Advanced Technology, Indore 452 013, India*
(Received 27 July 2000; published 12 January 2001)

An experimental study is presented on harmonic generation from solid surfaces using 27 ps Nd:glass laser pulses ($\lambda = 1053$ nm) in the intensity range of 10^{13}–10^{15} W cm^{-2}. Second, third, and fourth harmonics emitted in the specular reflection direction showed intensity scaling exponents of 1.5, 1.8, and 3.8 for an obliquely incident *p*-polarized laser beam, providing a conversion efficiency of 2×10^{-8}, 10^{-10}, and 5×10^{-12} at 10^{15} W cm^{-2}, respectively. Second and third harmonic radiation generated using an *s*-polarized pump was about 10 and 100 times smaller, respectively, compared to that for the *p*-polarized laser radiation. Faraday rotation observed in the reflected fundamental radiation can explain the relative harmonic yields for the *p* and *s* polarizations of the pump beam.

DOI: 10.1103/PhysRevE.63.026402 PACS number(s): 52.50.Jm, 42.65.Ky, 52.38.−r

I. INTRODUCTION

A number of theoretical and experimental studies [1–16] have been reported during the last decade on harmonic generation from solid surfaces using ultrashort laser pulses ranging from tens of femtoseconds up to a few picoseconds. Laser-matter interaction in this pulse duration regime is characterized by a steplike density profile where density drops from the solid density to that of the vacuum over a very small distance $L \ll \lambda$ (the wavelength of the laser radiation). Generation of odd as well as even harmonics in such cases has been explained as due to a strongly anharmonic motion of electrons across the sharp density step, e.g., as in the moving mirror model [11–13], or by considering the $\mathbf{v}\times\mathbf{B}$ Lorentz force at relativistic electron velocities for $I\lambda^2$ (I is the laser intensity) exceeding 10^{17} W cm^{-2} μm^2 [13–16]. Some common features observed in such interactions include a considerably larger efficiency of harmonic generation for *p*-polarized than for an *s*-polarized laser pump, and a smooth roll-off of the high order harmonic intensity. Further, while these harmonics appeared in the specular reflection direction for $I\lambda^2 \leqslant 10^{15}$–$10^{16}$ W cm^{-2} μm^2 [1,5,7,9,10], the emission became more isotropic at higher values of $I\lambda^2$ [4,7].

The situation is quite different for nanosecond long laser pulses where the density scale length is much larger than the laser wavelength ($L \gg \lambda$). In most experiments performed with obliquely incident, *p*-polarized Nd:glass nanosecond laser pulses with $I \leqslant 10^{15}$ W cm^{-2}, only second harmonic radiation was observed, e.g., as reported by Basov *et al.* [17]. The second harmonic was produced due to nonlinear interaction of the electromagnetic wave with a longitudinal Langmuir plasma wave or of two Langmuir waves in the vicinity of the critical density, and thus showed a scaling with laser intensity as I_L^2. Very high order (up to 46th) harmonics were first observed in nanosecond pulse CO_2 laser irradiation [18] at $\sim 10^{16}$ W cm^{-2}. These were explained [19] as arising from anharmonic motion of electrons across the steep density profile near the critical surface. The formation of a steep density gradient was attributed to the action of the ponderomotive force, which counteracts the plasma expansion. Harmonics up to fifth order were reported [20] in Nd:glass laser irradiation at an intensity of $\sim 10^{16}$ W cm^{-2} using 75 ps laser pulses. A common feature observed in such investigations was emission of harmonics over a broad angular range. However, this is undesirable since radiation confined to a narrow angular range (e.g., in the specular direction) is required to achieve high brightness. Further, the harmonic showed a rather poor dependence on the polarization of the incident laser beam. These effects were understood to occur due to rippling of the critical density surface by Rayleigh-Taylor-like instabilities as the expanding plasma is pushed back by the ponderomotive force [13–15]. Similar effects are also expected in ultrashort laser pulse irradiation in the presence of a prepulse [5,7], which may produce a long scale length underdense plasma.

From the above discussion, it is clear that both the laser intensity and pulse duration play an importance role in governing the processes involved in harmonic generation. In this work, we extend the temporal scale of the pump source to an intermediate range of a few tens of picoseconds, resulting in plasmas with density scale length of the order of the laser wavelength ($L \approx \lambda$). A smaller spatial extent of the underdense plasma would help to avoid or reduce the occurrence of Raylegh-Taylor instability over the short duration of the laser pulse. At the same time the plasma has a sufficiently low density (yet overdense) region permitting enhancement of the electric field amplitude [13,16], unlike solid densities which produce strong damping due to a large value of ω_p/ω_L (ratio of local plasma frequency and laser frequency). High order harmonics may therefore be expected in such plasmas even at moderate laser intensities. In this paper, we report an experimental study of harmonic generation from solid surfaces using prepulse-free Nd:glass laser pulses of 27 ps full width at half maximum (FWHM) in the intensity range of 10^{13}–10^{15} W cm^{-2}. Harmonic generation up to fourth order is observed in the specular direction. Measurements of the harmonic yields for *p* and *s*-polarization pumps, and their scaling with laser intensity are presented. The re-

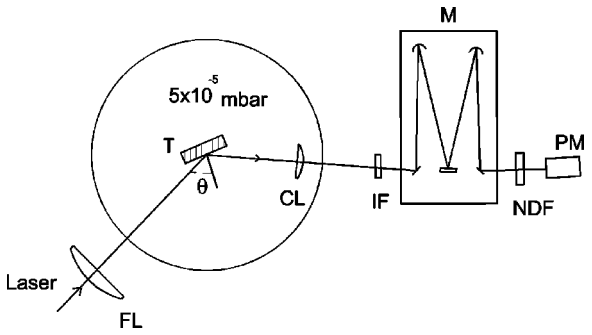

FIG. 1. A schematic of the experiment setup: FL, focusing lens; T, target; CL, collimator lens; IF, interference filters; M, monochromator; PM, photomultiplier.

sults are compared with those expected for the long and ultrashort pulse regimes.

II. DESCRIPTION OF EXPERIMENT

A 100 GW Nd:phosphate glass laser system ($\lambda = 1053$ nm) was used for harmonic generation from the surfaces. This laser system consisted of an active-passive mode-locked Nd:YLF oscillator, an electro-optic pulse selector, two double-pass amplifiers, two single-pass amplifiers, three vacuum spatial filters, and a Faraday isolator to block any backreflected laser beam. Single laser pulses of energy up to 2.5 J in 27 ps (FWHM) with a beam divergence angle of 175 μrad are available from this system. The laser beam was checked for any prepulses (due to leakage transmission of the rejected pulses of the mode-locked train from the pulse selector) and amplified spontaneous emission (ASE) from the amplifiers. The intensity contrast of the prepulses with the main laser pulse was measured to be better than 10^5. Thus prepulse intensity was $\leqslant 10^{10}$ W cm^{-2} at the maximum laser energy, and this is below the plasma formation threshold for picosecond laser pulses [6]. Further, the ASE also did not form any plasma from the target surface as checked by aborting the oscillator operation and firing all the amplifier stages. A Faraday rotator was also placed at the end of the laser chain to rotate the polarization of the output beam from *p* to *s* and vice versa. The depolarization factor of the laser radiation was smaller than 10^{-3}.

A schematic diagram of the experimental setup is shown in Fig. 1. The laser beam was focused using a 750 mm focal length lens on an aluminum target placed in a chamber evacuated to 5×10^{-5} mbar. The focal spot on the target was of an elliptical shape (due to non-normal incidence of the laser beam). For an angle of incidence of 67.5°, the major and minor dimensions of the focal spot were 120 μm and 45 μm, respectively. The target was prepared by coating 100 μm thick aluminum on optically polished planar glass plates. A fresh area on the target was used for each laser shot. A peak intensity of 1.5×10^{15} W cm^{-2} was estimated for the maximum output energy of the laser.

Reflected fundamental and harmonic radiations were collimated by a quartz lens and dispersed by a monochromator (CVI, model DK480). Appropriate broadband and interference filters were used to prevent undesirable plasma radiation at other wavelengths from reaching the detector. Photomultipliers were used for harmonic detection, and signals were displayed on Tektronix TDS-360 and LeCroy 9350A oscilloscopes. The overall rise time of the detection system was better than 3 ns. This was adequate to observe signal due to harmonics of the laser radiation distinctly separated from that due to radiation at the harmonic wavelengths emitted from the expanding plasma plume, which appeared as a broad peak later in time.

Measurements of harmonic intensity were performed for *p* and *s* polarizations of the pump beam for different values of the laser intensity in the range of 10^{13}–10^{15} W cm^{-2}. The following procedure was adopted to determine the conversion efficiency for different harmonics from the measured signals. The laser radiation at fundamental frequency was converted before the vacuum chamber to second, third, and fourth harmonics using potassium dihydrogen phosphate (KDP) crystals, and their energies were measured by using a standard energy meter. After decreasing their energy using calibrated bandpass and interference filters, different harmonics were made to propagate through the same detection channels as the harmonics produced from solid surface. Thus a calibration factor between the photomultiplier signal and the harmonic energy was established for the various harmonics.

III. RESULTS AND DISCUSSION

Second harmonic emission was observed in the direction of specular reflection for different values of laser intensity ranging from 10^{13} W cm^{-2} to 10^{15} W cm^{-2}. No second harmonic emission signal was observed at angles other than the specular reflection direction as checked by placing the collimating lens to collect radiation in directions away from specular. Further, measurements of the spatial shapes of the reflected laser radiation and the second harmonic showed that their divergences were nearly equal. The second harmonic signal in the specular reflection direction was fairly strong; so much so that a well-collimated second harmonic beam in the direction of specular reflection could be readily observed with the unaided eye. These observations are in agreement with earlier published work [5,9] using prepulse-free Nd:glass laser radiation up to the same maximum intensity of $\sim10^{15}$ W cm^{-2} as in our experiment but using much shorter pulses of 1 and 2.2 ps.

The occurrence of harmonic radiation predominantly in specular direction or over a broad angular range is governed by the shape of the critical density surface. Some processes, e.g., the ponderomotive force, lead to a growth of Rayleigh-Taylor instability resulting in distortions of the interface of the dense plasma [13–15] and consequent broadening of the angular spectrum of the harmonic emission. For instance, Chambers *et al.* [7] reported a change from specular harmonic emission to diffuse emission when $I\lambda^2$ in their experiment was increased from 10^{15} to 10^{16} W cm^{-2} μm^2. It was suggested that this change might have occurred due to the prepulse becoming sufficiently intense to produce a plasma ahead of the main laser pulse. A similar transition from specular to diffuse emission on introduction of a prepulse

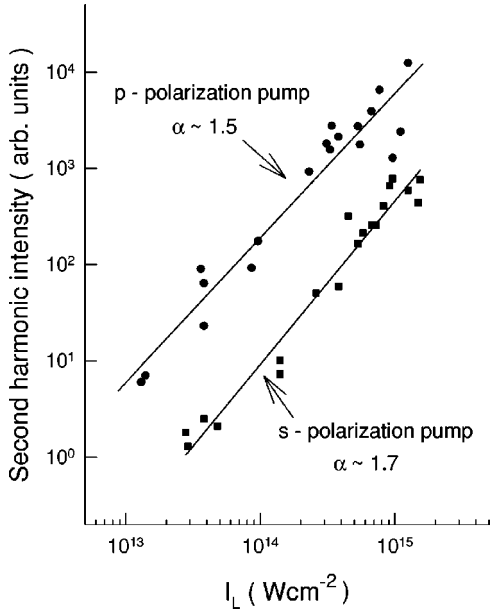

FIG. 2. Second harmonic intensity as a function of laser intensity for *p*- and *s*-polarized fundamental radiation.

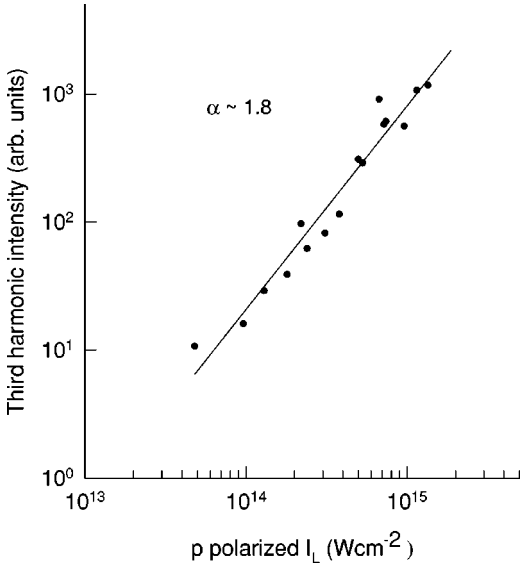

FIG. 3. Third harmonic intensity as a function of laser intensity for *p*-polarized pump beam.

was observed by Marjoribanks *et al.* [5]. It may be noted that even with low relative prepulse levels, at high intensities the temporal wings on the pulse may have sufficient intensity to preform a plasma at the target. The production of a long scale length underdense plasma region due either to a prepulse or sufficient intensity in the temporal wings of the pulse as discussed above, or that encountered in plasma formed by long pulse duration lasers, and its pushing back by the ponderomotive force, may lead to growth of hydrodynamic instabilities resulting in rippling of the critical density surface. This effect would become increasingly important as laser intensity is increased, particularly for $I\lambda^2 \geqslant 10^{15}$ W cm^{-2} μm^2. The absence of any diffuse harmonic emission in our experiments would indicate that the laser pulse interacted with a sharp dense-plasma–vacuum interface. A quantitative estimate of the density scale length can be obtained from a measurement of the optimum angle of incidence for maximum absorption of a *p*-polarized laser beam. Since our experiment is performed at small intensity of 10^{13}–10^{15} W cm^{-2}, the density scale length is expected to be comparable to or even smaller than the laser wavelength λ due to slower plasma expansion.

The second harmonic intensity as a function of laser intensity for *p* and *s* polarized fundamental radiation is shown in Fig. 2. It is seen that harmonic conversion for the *p*-polarized pump radiation is much higher than that for the *s*-polarized one. The data can be represented by a power law of the form $I_{2\omega} \propto I_{\omega}^{\alpha}$, where the intensity scaling exponent α is 1.5 and 1.7 for *p* and *s* polarizations, respectively. The conversion efficiency for second harmonic was determined to be 2×10^{-8} at the maximum laser intensity of $\sim10^{15}$ W cm^{-2} for the *p*-polarized pump radiation, and about 10 times smaller for the *s*-polarized one. Next, Fig. 3 and Fig. 4 show the dependence of the third and fourth harmonic intensity, respectively, on laser intensity for *p*-polarized fundamental radiation. The intensity scaling exponents α observed for the two harmonics are 1.8 and 3.8, respectively. The conversion efficiency for the third and fourth harmonics for the *s*-polarized radiation relative to that for the *p*-polarized beam was much smaller in comparison to that for the second harmonic. Specifically, the ratio of third harmonic conversion efficiency for the *p* and *s* polarizations was observed to be more than 100. Further, we did not observe any fourth harmonic radiation signal in the case of the *s*-polarized laser pump, primarily because the signal was below the detection threshold of our detection system. The conversion efficiency for the third and fourth harmonics for a *p*-polarized fundamental beam at 10^{15} W cm^{-2} was measured to be $\sim10^{-10}$ and 5×10^{-12}, respectively. The conver-

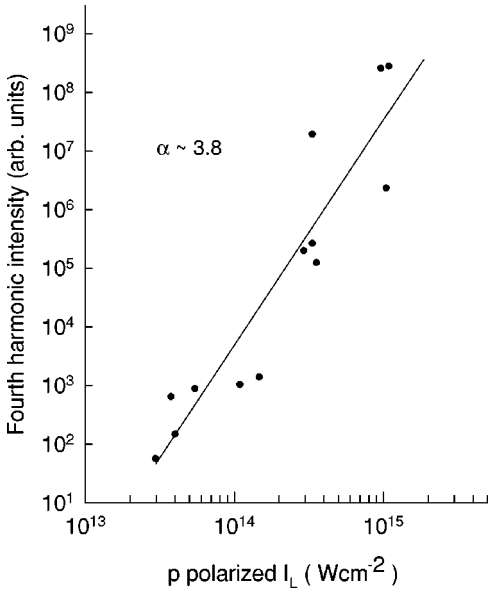

FIG. 4. Fourth harmonic intensity as a function of laser intensity for *p*-polarized pump beam.

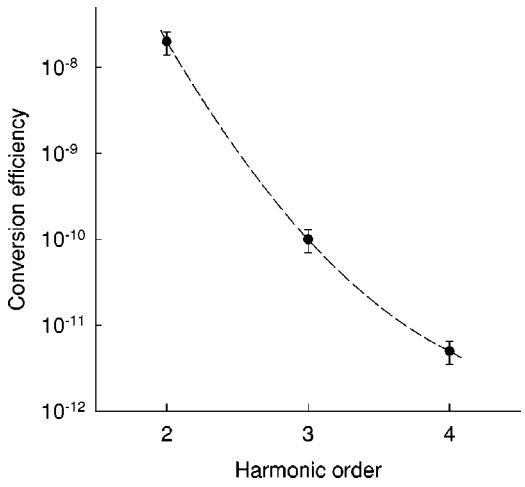

FIG. 5. Conversion efficiency for different harmonic orders at a laser intensity of 10^{15} W cm^{-2}. (The dashed line shown is only to guide the eye.)

sion efficiency for different harmonic orders is depicted in Fig. 5.

Our measurements of relative yield of the second harmonic for *s* and *p* polarized pump beams are in agreement with those reported by Losev and Soskov [6], who observed this ratio to be ~ 0.1 for 0.8 ps Nd:glass laser pulses at 10^{15}–10^{16} W cm^{-2}. However, the ratio of harmonic yields for *s* and *p* polarized pump beam observed in our experiment was much higher than that of 10^{-3} reported by von der Linde *et al.* [21] in experiments performed using 350 fs Ti-sapphire laser pulses at 10^{16} W cm^{-2}. Since harmonic emission in the specular direction is linked to the fundamental beam reflected in the same direction, we have measured the polarization characteristics of the reflected pump radiation. A Glan prism was used to analyze the polarization composition of the reflected beam, and the energy of the two orthogonal components was measured by a pair of calibrated energy meters.

Figure 6 shows the fraction of *p*-polarized component in the specularly reflected fundamental for *s*-polarized pump

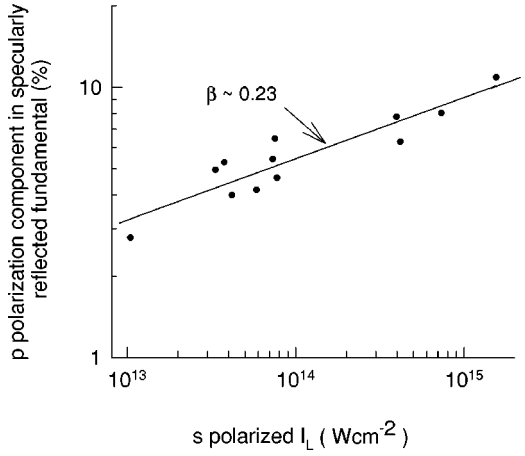

FIG. 6. Fraction of *p*-polarized component present in specularly reflected fundamental radiation for an *s*-polarized pump beam.

radiation as a function of laser intensity. It is noted that this fraction increases from about 3% at 10^{13} W cm^{-2} to about 10% at 10^{15} W cm^{-2}. This amount is significant as the extent of depolarization of the incident laser beam was only $\sim 0.1\%$. Further, the fraction of *p*-polarized component in the reflected fundamental radiation (for the *s*-polarized pump beam) showed a scaling of the form I_L^{β}, where $\beta \approx 0.23$. As discussed later, an orthogonal *p*-polarized component may appear because of Faraday rotation of the fundamental *s*-polarized beam due to self-generated magnetic fields in the plasma [22], and this can explain reasonably well the difference in the data on scaling exponent and relative yield of second harmonic emission for the *s*-polarized pump as compared to that for the *p*-polarized beam, shown in Fig. 2.

In order to explain the observed behavior of harmonic emission, viz., scaling laws with laser intensity, relative yields for different harmonic orders, and the ratio of harmonic yields for *p*- and *s*-polarized pump beams, we consider the two main mechanisms of harmonic generation in plasmas produced from solid surfaces. These are (1) production of nonlinear current in the critical density region, and (2) anharmonic motion of electrons across a steep density gradient. A third mechanism of harmonic generation through the $\mathbf{v}\times\mathbf{B}$ Lorentz force which becomes operative in the relativistic regime for $I\lambda^2 \geqslant 10^{17}$–$10^{18}$ W cm^{-2} μm^2 is not of much significance for the present investigation, performed up to a maximum laser intensity of 10^{15} W cm^{-2}. In reference to the first mechanism, second harmonics in the specular direction can occur through nonlinear interaction of a transverse electromagnetic wave with a longitudinal plasma wave [17,21,23]. In the vicinity of the critical density surface ($\omega = \omega_p$), these two modes can mix to produce second harmonic radiation through the nonlinear current $j_{2\omega}$ at the second harmonic frequency. This current can be expressed [24] in the form

$$j_{2\omega} \propto \left[\frac{\omega_p^2}{4\omega^2} \nabla E^2 + \frac{\omega_p^2}{\omega^2 - \omega_p^2} E(E \cdot \nabla \ln n_0) \right]. \qquad (1)$$

It is clear from the above expression that a density gradient in the plasma is necessary for harmonic generation since for a uniform density plasma the first term (ω_p^2 is $\propto n_0$) is irrotational and the second term is zero.

A qualitative insight into the role of the pump beam polarization in harmonic conversion can also be realized from expression (1). For an *s*-polarized pump beam, the second term makes no contribution to the nonlinear current since the laser electric field is perpendicular to the density gradient. On the other hand, for an obliquely incident *p*-polarized beam, this term makes a large contribution due to its resonance character at the critical density n_{cr}. Thus second harmonic generation is expected to be much larger for a *p*-polarized pump than for the *s*-polarized one. Further, while much of the 2ω radiation may be reflected in the specular direction, a part would propagate up the density profile and resonantly excite a longitudinal plasma wave at $4n_{cr}$. Nonlinear mixing of the electromagnetic and longitudinal plasma waves would then produce higher harmonics. The harmonic

intensity should therefore scale as I_L^n where n is the harmonic order. Moreover, since generation of the next higher order harmonic requires nonlinear interaction with the lower order harmonics, the conversion efficiency of higher order harmonics would decrease rather sharply with increasing order.

The second mechanism of harmonic generation is based on anharmonic motion of electrons across a steep density gradient of the surface plasma produced by an ultrashort laser pulse [1,19]. In this case, the density scale length L is much smaller than the laser wavelength ($L \leqslant 0.1\lambda$). For high values of $I\lambda^2$, the oscillation amplitude of electrons may exceed the density scale length. This introduces anharmonicity in the electron motion due to the large difference in the restoring force on the two sides of the steplike density gradient between the solid density and the vacuum level. The anharmonic response of the interface electrons gives rise to radiation at higher harmonics of the driving fundamental pump beam. Since anharmonicity is governed by the electron excursion relative to the density scale length, the intensity of the various order harmonics will be governed by the steepness of the density gradient and $I\lambda^2$ of the pump radiation. For a sharp density gradient, the intensity of higher order harmonics is expected to roll off smoothly.

Several characteristics of high order harmonic emission using ultrashort laser pulses have been explained by a moving mirror model in which the plasma-vacuum interface acts like a periodically moving mirror with a phase modulation [11–13]. Recent computer simulations have also predicted that there is no upper cutoff for the highest order of harmonic emission [15,16]. Further, since electron excursion across the density step is the basis of this mechanism, polarization of the driving beam plays an important role. The process occurs naturally for an obliquely incident *p*-polarized laser beam since the electric field vector has a component along the direction of the target normal. On the other hand, for an *s*-polarized pump, since the electric field is perpendicular to the density gradient, no significant electron excursion will occur across the density step for the nonrelativistic regime ($I\lambda^2 \ll 10^{17}$–10^{18} W cm^{-2} μm^2). Various polarization selection rules for high order harmonic conversion have also been predicted from theoretical considerations [8,12,13], and some measurements of harmonic polarization have been reported [21,25].

We now analyze our results in terms of the above two mechanisms. It may be noted that, for the laser pulse duration of 27 ps in our study, the ratio of density gradient scale length and laser wavelength, i.e., $L/\lambda \approx v_{exp} \times t_p/\lambda$, would be about 1 to 3 for the intensity range of 10^{13}–10^{15} W cm^{-2}. This is considerably larger than the steplike density gradient encountered in ultrashort laser pulse interaction ($L/\lambda \leqslant 0.1$) for which the second mechanism is operative, but much shorter than those encountered in the long pulse (nanosecond) irradiation ($L/\lambda \sim 10$ to 100). While all our observations can not be attributed to either one of the two mechanisms, their main features can jointly explain most of our results. For instance, while the first mechanism predicts a harmonic intensity scaling with laser intensity with an intensity scaling exponent α equal to the order of the harmonic, the second mechanism predicts a linear scaling. The latter is so because the electron current driven by the incident laser beam is proportional to the strength of the laser electric field. The intensity scaling exponents α of 1.5 for the second harmonic and 1.8 for the third harmonic observed in our experiment lie nearly midway between the power scaling exponents predicted by the two mechanisms. Further, we may compare these scalings with those observed in some earlier studies. For instance, while a scaling relation of $I_{2\omega} \propto I_\omega^{2.6}$, closer to the prediction of the first mechanism, was reported in Ref. [21] for plasmas produced by 350 fs laser pulses at 10^{16} W cm^{-2}, a nearly linear scaling of $I_{2\omega,3\omega} \propto I_\omega^{1.2}$ was observed in plasmas produced by 0.8 ps Nd:glass laser pulses in the intensity range of 10^{15}–10^{16} W cm^{-2} [6], as expected from the second mechanism. Next, the power scaling exponent of 3.8 observed for the 4ω radiation in our study is close to the prediction of the first mechanism. This may be expected since high order harmonic generation will be relatively less favorable through the second mechanism for the case of a longer density scale length plasma produced using multipicosecond laser pulses.

Next, we discuss the harmonic generation efficiency. As seen from Fig. 5, the conversion efficiency decreases by a factor of 4×10^3 in going from the second to the fourth harmonic, which is fast in comparison to the gradual roll off expected for ultrashort pulse interactions. For instance, in Ref. [6], second and third harmonic conversion efficiencies for *p*-polarized Nd:glass laser pulses of 0.8 ps at 10^{15}–10^{16} W cm^{-2} were observed to be 1.5×10^{-5} and 8×10^{-6}, respectively. Next, the second harmonic conversion efficiency ($\eta_{2\omega}$) in our study is similar to that reported by Ishizawa *et al.* [9] in experiments using 2.2 ps Nd:glass laser pulses, but it is lower compared to results of some other studies, e.g., $\eta_{2\omega}$ was observed to be $\approx 2.5 \times 10^{-6}$ in 350 fs pulse irradiation at 10^{15} W cm^{-2} [21]. However, no earlier study in the long pulse regime reported specular emission of third and fourth harmonic radiations for $I\lambda^2$ in the range of 10^{13}–10^{15} W cm^{-2} μm^2. It is thus reasonable to infer that a rather sharp density gradient ($L \approx \lambda$) is responsible for observation of these harmonics in the present study. The important role of a steep density gradient was demonstrated from generation of third and fourth harmonics in ultrashort pulse irradiation of solid surfaces at intensities well below the threshold for plasma formation [2].

Next, we discuss the relative harmonic yield for *p*- and *s*-polarized pump radiation and their scaling with laser intensity. As predicted by both the mechanisms, *s*-polarized radiation should be rather ineffective for producing higher harmonics. A significant conversion for the *s*-polarized pump radiation may be understood, as stated earlier, from Faraday rotation of the laser radiation due to self-generated magnetic fields in the plasma [22]. It may be noted from Fig. 6 that, at the maximum laser intensity of 10^{15} W cm^{-2}, the *p*-polarized component constitutes about 10% of the specularly reflected fundamental radiation. This is not surprising as a polarization rotation angle of 22.5° was reported by Stamper and Ripin [22] in plasma produced using 100 ps Nd:glass laser pulses at a similar intensity of 10^{15} W cm^{-2}

and this rotation corresponds to the presence of $\sim 15\%$ of the orthogonal polarization component. It can therefore be inferred that in our experiment a rotation of the *s*-polarized pump beam occurred during its propagation through the plasma, producing a *p*-polarized component, which is then responsible for the observed harmonic conversion. The relative yields observed for the *s*- and *p*-polarized pump beams (Fig. 2) agree well with the fraction of *p*-polarized component in the reflected fundamental radiation. Next, this fraction increases with laser intensity, exhibiting a power scaling exponent $\beta \approx 0.23$ (Fig. 6). This, when combined with the intensity scaling exponent of 1.5 observed for the *p*-polarized pump beam, gives a power scaling exponent of 1.73 for the second harmonic for the *s*-polarized pump beam, in good agreement with the observed result. Ishizawa *et al.* [9] considered the possible role of self-generated magnetic fields to explain a relatively large yield for the *s*-polarized pump beam in their experiment. However, our measurements of the polarization composition of the specularly reflected fundamental radiation are able to quantitatively explain both the relative yield and the difference in the power scaling exponents for second harmonic generation for the *s*- and *p*-polarized pump radiation.

In conclusion, we have performed a study of harmonic generation from solid surfaces irradiated by 27 ps Nd:glass laser pulses in the intensity range of 10^{13}–10^{15} W cm^{-2}. Harmonic emission up to fourth order is observed in the specular reflection direction with conversion efficiencies of 2×10^{-8}, 10^{-10}, and 5×10^{-12} for second, third, and fourth harmonic, respectively, for a *p*-polarized pump beam at 10^{15} W cm^{-2}. Measurements of the scaling laws of harmonic intensity with laser intensity for various harmonic orders and different polarizations of the pump beam are analyzed by comparing with the expected behavior for two important mechanisms of harmonic emission, viz., generation of nonlinear currents and anharmonic motion of electrons across a sharp density gradient. A larger than expected relative conversion for the *s*-polarized pump in comparison to the *p*-polarized pump is explained as due to Faraday rotation of the pump beam by self-generated magnetic fields in the plasma. While a theoretical analysis including computer simulations may be necessary for a detailed quantitative analysis of the characteristics of the laser-plasma interaction involved, the various observations are reasonably well explained from simple considerations of different physical processes relevant to the harmonic emission.

ACKNOWLEDGMENTS

One of the authors (R.A.G.) would like to thank D. D. Bhawalkar for hospitality during his stay at the Center for Advanced Technology. He would also like to acknowledge the Third World Academy of Sciences for providing financial support.

[1] D. von der Linde *et al.*, Phys. Rev. A **52**, R25 (1995).
[2] G. Farkas *et al.*, Phys. Rev. A **46**, R3605 (1992).
[3] S. Kohlweyer *et al.*, Opt. Commun. **117**, 431 (1995).
[4] P. A. Norreys *et al.*, Phys. Rev. Lett. **76**, 1832 (1996).
[5] R. S. Marjoribanks, L. Zhao, G. Kulcsar, and F. W. Budnik, Bull. Am. Phys. Soc. **41**, 1424 (1996).
[6] L. L. Losev and V. I. Soskov, Kvant. Elektron. (Moscow) [Quantum Electron. **28**, 454 (1998)].
[7] D. M. Chambers *et al.*, Opt. Commun. **148**, 289 (1998).
[8] D. von der Linde, Appl. Phys. B: Lasers Opt. **68**, 315 (1999).
[9] A. Ishizawa *et al.*, IEEE J. Quantum Electron. **35**, 60 (1999).
[10] C. T. Hansen, S. C. Wilks, and P. E. Young, Phys. Rev. Lett. **83**, 5019 (1999).
[11] S. V. Bulanov, N. M. Naumova, and F. Pegoraro, Phys. Plasmas **1**, 745 (1994).
[12] D. von der Linde and K. Rzazewski, Appl. Phys. B: Lasers Opt. **63**, 499 (1996).
[13] R. Lichters, J. Meyer-ter-Vehn, and A. Pukhov, Phys. Plasmas **3**, 3425 (1996).
[14] S. C. Wilks, W. L. Kruer, and W. B. Mori, IEEE Trans. Plasma Sci. **21**, 120 (1993).
[15] P. Gibbon, Phys. Rev. Lett. **76**, 50 (1996).
[16] P. Gibbon, IEEE J. Quantum Electron. **33**, 1915 (1999).
[17] N. G. Basov *et al.*, Kvant. Elektron. (Moscow) **6**, 1829 (1979) [Sov. J. Quantum Electron. **9**, 1081 (1979)].
[18] R. L. Carman, C. K. Rhodes, and R. F. Benjamin, Phys. Rev. A **24**, 2649 (1981).
[19] B. Bezzerides, R. D. Jones, and D. W. Forslund, Phys. Rev. Lett. **49**, 202 (1982).
[20] E. A. McLean *et al.*, Appl. Phys. Lett. **31**, 825 (1977).
[21] D. von der Linde, H. Schulz, T. Engers, and H. Schuler, IEEE J. Quantum Electron. **28**, 2388 (1992).
[22] J. A. Stamper and B. H. Ripin, Phys. Rev. Lett. **34**, 138 (1975).
[23] R. Dragila, Phys. Rev. A **25**, 1127 (1982).
[24] Y. R. Shen, *The Principles of Nonlinear Optics* (Wiley, New York, 1984), p. 553.
[25] G. Veres *et al.*, Europhys. Lett. **48**, 390 (1999).